LWT - Food Science and Technology 149 (2021) 111857

Contents lists available at ScienceDirect

LWT

journal homepage: www.elsevier.com/locate/lwt

Water desorption isotherms of pork liver and thermodynamic properties

E.A. Sánchez-Torres, B. Abril, J. Benedito, J. Bon, J.V. García-Pérez *

UPV, Universitat Politècnica de València, Department of Food Technology, Camí de Vera, S/n, 46022, Valencia, Spain

ARTICLE INFO

Keywords:
Pork liver
Desorption isotherm
Thermodynamic properties
Isosteric heat
Entropy

ABSTRACT

For the first time, the relationship between equilibrium moisture content and water activity is reported for the desorption process in pork liver. For that purpose, a standardized conductivity hygrometer was used at four different temperatures (0, 10, 30 and 50 °C) over a wide range of water activity (0.999–0.103). Five models frequently found in the literature (GAB, Oswin, Henderson, Hasley and Ratti) were considered for the purposes of describing the experimental desorption. The GAB model emerged as the best option (explained variance 96.6%) for the physical and mathematical description of the water desorption isotherms in pork liver. The computed isosteric heat, entropy and Gibbs energy illustrated the high water-sorbent affinity, because of a considerable availability of strong sorption sites at low moisture contents.

The reported experimental desorption isotherms, and modeling results, are essentials for the optimal design of the drying process of pork liver, which is a necessary step for the further research addressing the extraction of the protein fraction from the dried product. Extraction and isolation of the protein fraction from pork liver could be considered a reasonable strategy considering the demand of protein materials and the high-environmental impact of the meat industry.

1. Introduction

Liver could be considered a relevant by-product of the pork industry. As a result of new consumption trends, there has been a decrease in household demand for pork liver, which nowadays is of low commercial value. Hence, pork liver is mainly used for liver paste products and animal feed, and less commonly, for the extraction of bioactive compounds, such as vitamin B12 or heparin in the pharmaceutical industry (Seong et al., 2014; Toldrá, Mora, & Reig, 2016). However, its high protein content (81.9%, d.b.) (Babicz et al., 2018) represents a potential source of technological proteins for use in the food industry. Functional proteins from pork liver could be obtained as an alternative to others that are widely used in the meat industry (Steen et al., 2016), such as dairy or vegetable proteins. In addition, its non-functional protein fraction could be hydrolyzed for the generation of bio-peptides with antioxidant or antimicrobial activity (Lafarga & Hayes, 2014; Mora, Reig, & Toldrá, 2014). Furthermore, pork liver presents a high concentration of Ferrochelatase, which is an enzyme that catalyzes the formation of Zinc protoporphyrin IX (ZnPP). ZnPP is a natural red pigment that, due to its stability to light and heat, might be useful as a means of improving the color of meat products, avoiding or minimizing the use of nitrites/nitrates (De Maere et al., 2017; Wakamatsu, Murakami, & Nishimura, 2015). In addition, the aforementioned potential uses of the pork liver would also positively impact on the sustainability of the pork-meat industry.

In order to extract the protein fraction of the pork liver, a prior dehydration stage may be required. Drying lengthens shelf life, facilitates storage conditions and reduces weight and volume in liver processing; however, it is important to investigate how a reduction in water content would affect protein quality. For the drying analysis and optimization of a particular food commodity, it is necessary to assess the relationship between its moisture content and the relative humidity of the atmosphere with which it is in equilibrium, is equivalent to the water activity. This relationship is known as a sorption isotherm and depends on the structure and composition of the food material, as well as the pressure and temperature. Specifically, water sorption isotherms can be generated from an adsorption (from dry to wet materials) or desorption process (from wet to dry materials), which usually differ showing a certain degree of hysteresis between both curves (Al-Muhtaseb, McMinn, & Magee, 2002; Mulet, García-Pascual, Sanjuán, & García-Reverter, 2002). Once the sorption isotherms have been determined at different temperatures, it is possible to compute different thermodynamic properties, such as the isosteric heat of sorption (enthalpy), the sorption entropy and Gibbs energy, which represent the energy

* Corresponding author.
E-mail address: jogarpe4@tal.upv.es (J.V. García-Pérez).

https://doi.org/10.1016/j.lwt.2021.111857
Received 3 May 2021; Received in revised form 27 May 2021; Accepted 31 May 2021
Available online 3 June 2021

associated with the rehydration or dehydration process and provide information on the molecular state of water within the dried product (Chen, 2006; Mbarek & Mihoubi, 2019; Sahu et al., 2018).

Water sorption isotherms have been reported for different protein matrices, such as beef (Ahmat, Bruneau, Kuitche, & Aregba, 2014; Kabil, Aktaş, & Balcı, 2012), pork (Clemente, Bon, Benedito, & Mulet, 2009; Comaposada, Gou, & Arnau, 2000), chicken (Delgado & Sun, 2002a), goat (Singh, Rao, Anjaneyulu, & Patil, 2006) or fish (Moraes & Pinto, 2012; Toujani, Hassini, Azzouz, & Belghith, 2011). Thus, water activity concepts have been used to explain physicochemical and microbiological changes in meat and fish (Taormina & Sofos, 2014, pp. 127–164). However, no references to the sorption isotherms of either pork liver or of other animal viscera have been reported, despite current interest in developing strategies for an efficient and sustainable use of meat by-products (Lee et al., 2020; Sarwar, Hussain, & Leghari, 2013; Yoon, Da Young Lee, Lee, & Hur, 2018). Therefore, the aim of this study is: (i) to provide experimental desorption isotherm data of pork liver at different temperatures (0, 10, 30 and 50 °C) and address the mathematical description using different models (GAB, Oswin, Henderson, Halsey and Ratti); (ii) to determine the main thermodynamic properties of the desorption process (isosteric heat, entropy and Gibbs energy).

2. Materials and methods

2.1. Experimental set up

Fresh pork liver was purchased from a local market (Valencia, Spain), frozen in a blast chiller at −18 °C for 240 min and stored until processing. Blast freezing allows the critical zone of water crystallization to be crossed quickly, thereby small ice crystals are formed and cellular osmotic dehydration is reduced. Thus, the formation of cell cracks and related damage is prevented, preserving the integrity of the food tissue and minimizing any possible effect on the moisture desorption (Kiani & Sun, 2011). The initial moisture content of the liver was determined according to AOAC method 950.46 B (AOAC, 2019) resulting in an average value of 73.04 ± 1.10% (w.b.). This figure is close to the moisture content found by Steen et al. (2016), which reported the following partial characterization of pork liver (w.b.): 72.4% moisture, 20.0% protein, 4.75% fat and 1.97% ash. The remaining part (0.88%) could be probably linked to the carbohydrates.

For the experimental determination of desorption isotherms, the liver was thawed at 4 °C for 24 h, ground (Type D56, Moulinex, Seb Group, France) and subsequently dried in monolayer (2–3 mm, ~10 g) at 60 °C using an air forced tray oven (Model FD115 Oven Forced Air, Binder, Tuttlingen, Germany) with a certain exchange to regenerate the inner air and keep the relative humidity below 5%. Thus, drying times from 1 to 48 h were applied in, at least, 19 independent drying experiments in order to reach a wide range of moisture contents. The partially dried samples were ground again and kept in airtight jars at 4 °C for 24 h to homogenize the moisture content, before measuring water activity and moisture content.

The water activity of each sample was measured in triplicate using a standardized conductivity hygrometer (Model AW Sprint TH 500, Novasina, Pfäffikon, Switzerland) at four different temperatures (0, 10, 30 and 50 °C). The equipment was previously calibrated, according to the calibration procedure of the equipment manufacturer, using the following salts: LiCl, $MgCl_2$, $Mg(NO_3)_2$, NaCl, $BaCl_2$ and $K_2Cr_2O_7$. Once the water activity measurement was concluded, the moisture content of each sample was determined in triplicate following the aforementioned AOAC method 950.46 B, which consists of drying the sample at 105 °C until constant weight (24 h). Using this methodology, which has been validated for other products (Fontana Jr. & Carter, 2020), nineteen experimental points (water activity/moisture content) were obtained for each temperature.

2.2. Modeling desorption isotherms

Five models that are widely used in food technology (GAB, Oswin, Henderson, Hasley and Ratti) were used to describe the desorption isotherms mathematically. In the first four models, the moisture content is described as a function of water activity and temperature, while in the Ratti model, the water activity is a function of moisture content and temperature.

The physical meaning and simplicity of the Guggenheim-Anderson-De Boer (GAB) model (Eq. (1)) (Anderson, 1946) makes it highly suitable for the purposes of describing and interpreting water sorption isotherms in foodstuffs. In addition, the GAB model has exhibited a good fitting capacity for wide ranges of moisture content (W), water activity (a_w) and temperature. The equation was recommended by the European Project COST90 (European Cooperation in Scientific and Technical Research) to describe moisture isotherms in food products (Robertson & Lee, 2021; Staudt, Tessaro, Marczak, Soares, & Cardozo, 2013).

$$W = \frac{W_m C K a_w}{(1 - K a_w)[1 + (C - 1) K a_w]} \tag{1}$$

where C and K can be written as temperature dependent functions using Arrhenius-type relationships, Eqs. (2) and (3).

$$C = C_0 \exp\left(\frac{\Delta H_C}{RT}\right) \quad \text{where} \quad \Delta H_C = H_m - H_n \tag{2}$$

$$K = K_0 \exp\left(\frac{\Delta H_K}{RT}\right) \quad \text{where} \quad \Delta H_K = L_v - H_n \tag{3}$$

Oswin (Chen, 1988), Henderson (Thompson, Peart, & Foster, 1968), Hasley (Iglesias & Chirife, 1976) and Ratti (Khalloufi, Giasson, & Ratti, 2000) models are described by Eqs. (4)–(7), respectively.

$$W = (A_{Os} + B_{Os} T)\left(\frac{a_w}{1 - a_w}\right)^{C_{Os}} \tag{4}$$

$$W = \left[-\frac{1}{A_H (T + C_H)} \ln(1 - a_w) \right]^{\frac{1}{B_H}} \tag{5}$$

$$W = \left[-\frac{\exp(C_{Ha} + B_{Ha} T)}{\ln(a_w)} \right]^{\frac{1}{A_{Ha}}} \tag{6}$$

$$\ln(a_w) = -k_1 W^{k_2} + k_3 \exp(-k_4 W) \ln(P_s)\ W^{k_5} \tag{7}$$

The temperature effect is introduced in Eq. (7) through the saturation vapor pressure term (P_s), which was calculated from the Antoine equation for pure water (Eq. (8)) (Poling, Prausnitz, & O'Connell, 2001).

$$\log_{10} P_s = a - \frac{b}{T + c} \quad \text{where} \quad \begin{array}{l} a = 10.11564 \\ b = 1687.537 \\ c = -42.98 \end{array} \tag{8}$$

2.3. Determination of the isosteric heat of desorption

The isosteric heat of desorption (Q_s, Eq. (9)) can be used to estimate the energy requirements of the drying process and represents the addition of the net isosteric heat of desorption (q_{sn}) to the latent heat of the vaporization of water (L_v). Thus, the net isosteric heat of desorption is interpreted as the binding energy between water molecules and the solid matrix in foodstuffs (Kaymak-Ertekin & Gedik, 2004).

$$Q_s = q_{sn} + L_v \tag{9}$$

$$\left[\frac{d \ln(a_w)}{dT}\right]_W = \frac{q_{sn}}{RT^2} \tag{10}$$

From the Clausius-Clapeyron equation (Eq. (10)), two methods were used to assess the net isosteric heat of desorption for a specific moisture

content (Chen, 2006; Haque, Shimizu, Kimura, & Bala, 2007):

1 Graphical method: The integration of Eq. (10) is as follows:

$$\ln(a_w) = -\left(\frac{q_{sn}}{R}\right)\frac{1}{T} + \text{constant} \tag{11}$$

The value of q_{sn} is calculated from the slope of Eq. (11), plotting $\ln(a_w)$ vs $1/T$. This procedure requires data from at least three experimental temperature levels.

2. Integral method: By integrating Eq. (10) between two particular temperatures (T_1 and T_2), q_{sn} can be inferred from the following expression:

$$q_{sn} = R\left(\frac{T_1\, T_2}{T_2 - T_1}\right)\ln\left(\frac{a_{w2}}{a_{w1}}\right) \tag{12}$$

where a_{wi} is the measurement of water activity at temperature T_i. Hence, measurements are required at only two temperatures.

Eq. (10) is based on the assumption that q_{sn} is constant with temperature. However, despite the fact that this has frequently been accepted, it is controversial since it may depend on the food material itself (Mulet et al., 2002). If the net isosteric heat of desorption for pork liver is independent of temperature, at least in the experimental range explored, both methods (graphical and integral) should provide similar values of q_{sn} (Iglesias, Chirife, & Fontan, 1989).

The Riedel equation (Eq. (13)) (Riedel, 1977) adequately describes the influence of temperature on water activity. By combining and rearranging Eqs. (12) and (13), another expression for estimating the net isosteric heat of desorption can be computed (Eq. (14)) (García-Pérez et al., 2008).

$$\ln\left(\frac{a_{w2}}{a_{w1}}\right) = A_r \exp(-B_r W)\left(\frac{1}{T_1} - \frac{1}{T_2}\right) \tag{13}$$

$$q_{sn} = A_r\, R \exp(-B_r W) \tag{14}$$

2.4. Determination of Gibbs energy and the desorption entropy

The change in Gibbs free energy (ΔG) can be used to assess the affinity between sorbent and water, and was calculated for each temperature using Eq. (15) (Yogendrarajah, Samapundo, Devlieghere, De Saeger, & De Meulenaer, 2015). Negative values of ΔG are associated with spontaneous exothermic processes, while positive values are characteristic of non-spontaneous endothermic processes. Since adsorption is essentially exothermic and desorption is mainly endothermic (Rizvi, 2014), if an adsorption process is analyzed, Eq. (15) should be used without the negative sign, due to the negative value of $\ln a_w$.

$$\Delta G = -RT \ln a_w \tag{15}$$

At constant temperature and pressure, the change in Gibbs free energy is defined by Eq. (16) (Green & Southard, 2019). For a desorption process, the enthalpy change (ΔH) is positive and equal to the net isosteric heat of desorption (q_{sn}), since heat is absorbed by the system. Thus, the sorption entropy change (ΔS) was computed by Eq. (17) for each temperature (Fakhfakh, Mihoubi, & Kechaou, 2018). If heat is released by the system, as in an adsorption process, q_{sn} should be negative.

$$\Delta G = \Delta H - T\Delta S \tag{16}$$

$$\Delta S = \frac{q_{sn} - \Delta G}{T} \tag{17}$$

The sorption entropy change is related to the degree of disorder or randomness (spatial arrangement) existing in the water-sorbent system and is proportional to the number of available sorption sites corresponding to a specific energy level (Khiari, Zemni, Maury, & Mihoubi, 2020).

2.5. Parameter estimation and statistical analysis

The model parameters were identified using an optimization procedure minimizing the sum of the squared residuals (Eq. (18)). For that purpose, the generalized reduced gradient (GRG) optimization method, available in the Microsoft Excel spreadsheet from Microsoft Office 2019 Professional Plus, was used.

$$\mathrm{F_{obj}} = \sum_{i=1}^{n}\left(y_{i\ exp} - y_{i\ calc}\right)^2 \tag{18}$$

The accuracy of fit was evaluated by computing the explained variance (VAR) (Eq. (19)) (Lipson & Sheth, 1973). Meanwhile, the plot of the residuals ($y_{i\ exp} - y_{i\ calc}$) against the independent variable (Staudt et al., 2013) was analyzed to identify the appearance of patterns.

$$\mathrm{VAR} = \left(1 - \frac{S_{yx}^2}{S_y^2}\right)100 \tag{19}$$

The standard deviation of the sample (S_y) and the standard deviation of the estimation (S_{yx}) are defined by Eqs. (20) and (21), respectively.

$$S_y = \sqrt{\frac{1}{n-1}\sum_{i=1}^{n}\left(y_{i\ exp} - \overline{y_{exp}}\right)^2} \tag{20}$$

$$S_{yx} = \sqrt{\frac{1}{n-m}\sum_{i=1}^{n}\left(y_{i\ exp} - y_{i\ calc}\right)^2} \tag{21}$$

The VAR represents the relative variance explained by the model with respect to the total variance, and it ranges from 0% to 100%. Moreover, the fit is considered meaningful when the residuals are caused only by random errors. These errors are assumed to be independent with a zero mean and constant variance and arranged in a normal distribution. If the residual plots show a clear pattern, the model should be rejected (Chen & Morey, 1989; Kaleemullah & Kailappan, 2004; Menkov, 2000).

3. Results and discussion

3.1. Experimental isotherms

Experimental values for desorption isotherms at different temperatures are shown in Table 1 and plotted in Fig. 1. For a given moisture content, water activity can be observed to increase slightly in line with temperature throughout the moisture range analyzed, common behavior in many food commodities. This fact implies that if the water activity is maintained constant, an increase in temperature causes a decrease in the amount of sorbed water. Iglesias and Chirife (1982) considered this aspect to indicate that the food matrix is becoming less hygroscopic as temperature increases. However, the temperature effect found on desorption isotherms for pork liver seems milder than in other products as is illustrated in Fig. 1.

Brunauer, Deming, Deming, and Teller (1940) classified sorption isotherms into five general types, and according to this classification, the sorption curves obtained are type II sigmoid in shape. This pattern presents a gradual rise in moisture content at low water activities followed by a sharp increase at high water activities. Similar behavior was observed for the isotherms of raw pork meat (Comaposada et al., 2000), beef (Ahmat et al., 2014; Aykın-Dinçer & Erbaş, 2018), chicken (Delgado & Sun, 2002a) or goat (Singh et al., 2006), as well as for fresh fish (Moraes & Pinto, 2012; Ponwiboon & Rojanakorn, 2017). It is worth mentioning that processing the raw meat, by cooking or salting, leads to a modification of the sorption process, shifting the curves from type II to III (Aykın-Dinçer & Erbaş, 2018; Betiol et al., 2020; Delgado & Sun, 2002b). Therefore, the desorption process of pork liver behaved

Table 1
Experimental equilibrium moisture content and water activity at 0, 10, 30 and 50 °C for pork liver (average values ± standard deviations).

W (d.b.)	a_w			
	0 °C	10 °C	30 °C	50 °C
0.571 ± 0.029	0.957 ± 0.003	0.965 ± 0.002	0.990 ± 0.004	0.999 ± 0.001
0.366 ± 0.008	0.886 ± 0.010	0.903 ± 0.008	0.921 ± 0.009	0.928 ± 0.006
0.213 ± 0.008	0.781 ± 0.005	0.804 ± 0.002	0.823 ± 0.004	0.832 ± 0.002
0.218 ± 0.002	0.775 ± 0.004	0.785 ± 0.007	0.800 ± 0.003	0.812 ± 0.002
0.205 ± 0.005	0.720 ± 0.007	0.733 ± 0.003	0.761 ± 0.009	0.786 ± 0.005
0.152 ± 0.002	0.662 ± 0.008	0.676 ± 0.001	0.718 ± 0.001	0.761 ± 0.006
0.193 ± 0.002	0.553 ± 0.005	0.586 ± 0.005	0.637 ± 0.001	0.654 ± 0.003
0.148 ± 0.010	0.468 ± 0.002	0.463 ± 0.001	0.522 ± 0.008	0.585 ± 0.006
0.097 ± 0.003	0.453 ± 0.007	0.457 ± 0.001	0.468 ± 0.001	0.490 ± 0.007
0.109 ± 0.004	0.432 ± 0.007	0.448 ± 0.003	0.463 ± 0.006	0.475 ± 0.002
0.072 ± 0.002	0.407 ± 0.008	0.429 ± 0.010	0.437 ± 0.001	0.468 ± 0.004
0.113 ± 0.012	0.403 ± 0.001	0.424 ± 0.001	0.432 ± 0.006	0.459 ± 0.002
0.128 ± 0.018	0.373 ± 0.005	0.411 ± 0.009	0.427 ± 0.009	0.451 ± 0.006
0.081 ± 0.001	0.364 ± 0.002	0.389 ± 0.004	0.415 ± 0.005	0.450 ± 0.003
0.078 ± 0.004	0.339 ± 0.006	0.367 ± 0.005	0.396 ± 0.006	0.432 ± 0.001
0.073 ± 0.002	0.338 ± 0.005	0.361 ± 0.009	0.381 ± 0.004	0.378 ± 0.005
0.052 ± 0.001	0.219 ± 0.003	0.221 ± 0.002	0.249 ± 0.004	0.290 ± 0.003
0.053 ± 0.003	0.182 ± 0.002	0.205 ± 0.010	0.224 ± 0.002	0.278 ± 0.001
0.026 ± 0.003	0.103 ± 0.006	0.139 ± 0.001	0.160 ± 0.007	0.178 ± 0.003

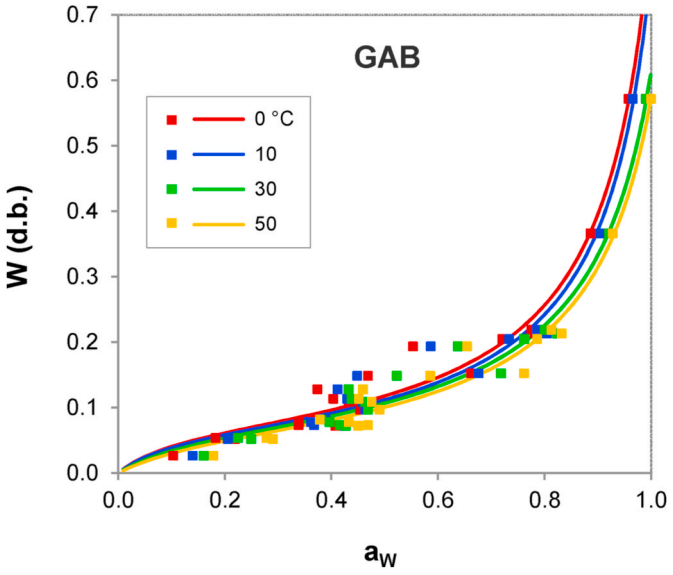

Fig. 1. Experimental desorption isotherms of pork liver and GAB model at 0, 10, 30 and 50 °C.

similarly to that of other raw animal products. In this sense, it must be once again mentioned that no references were found either to liver or to similar animal viscera in the literature.

Raw pork liver presents a high amount of available water, as is reflected by the fact that the reduction of the water activity to figures lower than 1 occurred at a relatively low equilibrium moisture contents (around 36% w. b.). Thus, a large amount of water, from the initial moisture content of 73% w. b. to 36% w. b., is highly available for degradation reactions, which explains the short shelf life of this food material. In addition, this fraction of water should present a weak bonding to the solid food matrix, which would have further implications in the drying process.

3.2. Modeling desorption isotherms

Experimental desorption isotherms were separately modeled at different temperatures using the GAB equation (Eq. (1)). The explained variance (VAR) of each fit was higher than 96.0% in all cases, which could be appropriate when considering the high experimental variability found. The estimated model parameters are shown in Table 2, while the simulated curves are plotted in Fig. 1. The parameters C and K tended to decrease as the temperature rose, as has been previously observed in other products, such as spray dried tomato pulp (Goula, Karapantsios, Achilias, & Adamopoulos, 2008), corn and potato starches (Al-Muhtaseb, McMinn, & Magee, 2004; Peng, Chen, Wu, & Jiang, 2007) or beef (Kabil et al., 2012). These results are consistent with the definition of the GAB model in which C and K depend on the temperature through Arrhenius-type relationships (Eqs. (2) and (3) respectively). In addition, the monolayer moisture content (W_m) reflected a slight decrease as the temperatures rose. Thus, it ranged from 0.071 at 0 °C to 0.065 d.b. at 50 °C, showing an average value of 0.068 ± 0.002 d.b. Different studies have reported the same fact when analyzing desorption processes; thus, the following W_m ranges (d.b.) have been found for different raw meat products: pork, 0.061–0.056 at 25–40 °C (Clemente et al., 2009), beef, 0.096–0.056 at 30–50 °C (Ahmat et al., 2014), chicken, 0.097–0.076 at 4–30 °C (Delgado & Sun, 2002a), and goat, 0.065–0.036 at 10–50 °C (Singh et al., 2006). From an adsorption process, Shi, Lin, Zhao, Zhang, and Wang (2016) identified values that ranged from 0.082 to 0.061 between 5 and 45 °C, working with freeze-dried *Penaeus vannamei* meat (shrimp). Thereby, the W_m figures found in this study are close to the ones reported in the literature for raw meat products.

In order to consider the influence of temperature, the experimental desorption isotherms were modeled with the GAB (Eqs. (1)–(3)), Oswin (Eq. (4)), Henderson (Eq. (5)), Hasley (Eq. (6)) and Ratti (Eqs. (7) and (8)) equations. The results of the modeling are shown in Table 3. The GAB, Henderson and Ratti models presented a random distribution in the residual plots (Figs. 2 and 3), as well as an explained variance (VAR) of over 90.0% in every case. For the Oswin and Hasley models, residuals presented clear patterns (Fig. 2), which makes its further use unfeasible. Fig. 4 shows the computed isotherms at different temperatures using Henderson and Ratti models, in a similar way that Fig. 1 for GAB model. Henderson model is more sensitive to the effect of the temperature than

Table 2
Identified GAB model parameters at constant temperature and explained variance (VAR).

T (°C)	W_m (d.b.)	C	K	VAR (%)
0	0.071	10.64	0.916	96.3
10	0.067	10.91	0.913	96.1
30	0.068	8.51	0.891	96.8
50	0.065	7.47	0.888	96.7

Table 3
Estimated model parameters and statistics.

Model	Parameters					VAR (%)	Residual plot
GAB	W_m	C_0	ΔH_C	K_0	ΔH_K	96.6	Random
	0.068	0.11	$1.07{\cdot}10^4$	0.69	$6.51{\cdot}10^2$		
Oswin	A_{Os}	B_{Os}	C_{Os}			79.8	Patterned
	0.65	−0.002	0.32				
Henderson	A_H	B_H	C_H			94.0	Random
	0.08	1.19	−185.8				
Hasley	A_{Ha}	B_{Ha}	C_{Ha}			73.4	Patterned
	3.02	−0.04	5.50				
Ratti	k_1	k_2	k_3	k_4	k_5	90.9	Random
	0.03	−1.52	0.09	31.28	−0.75		

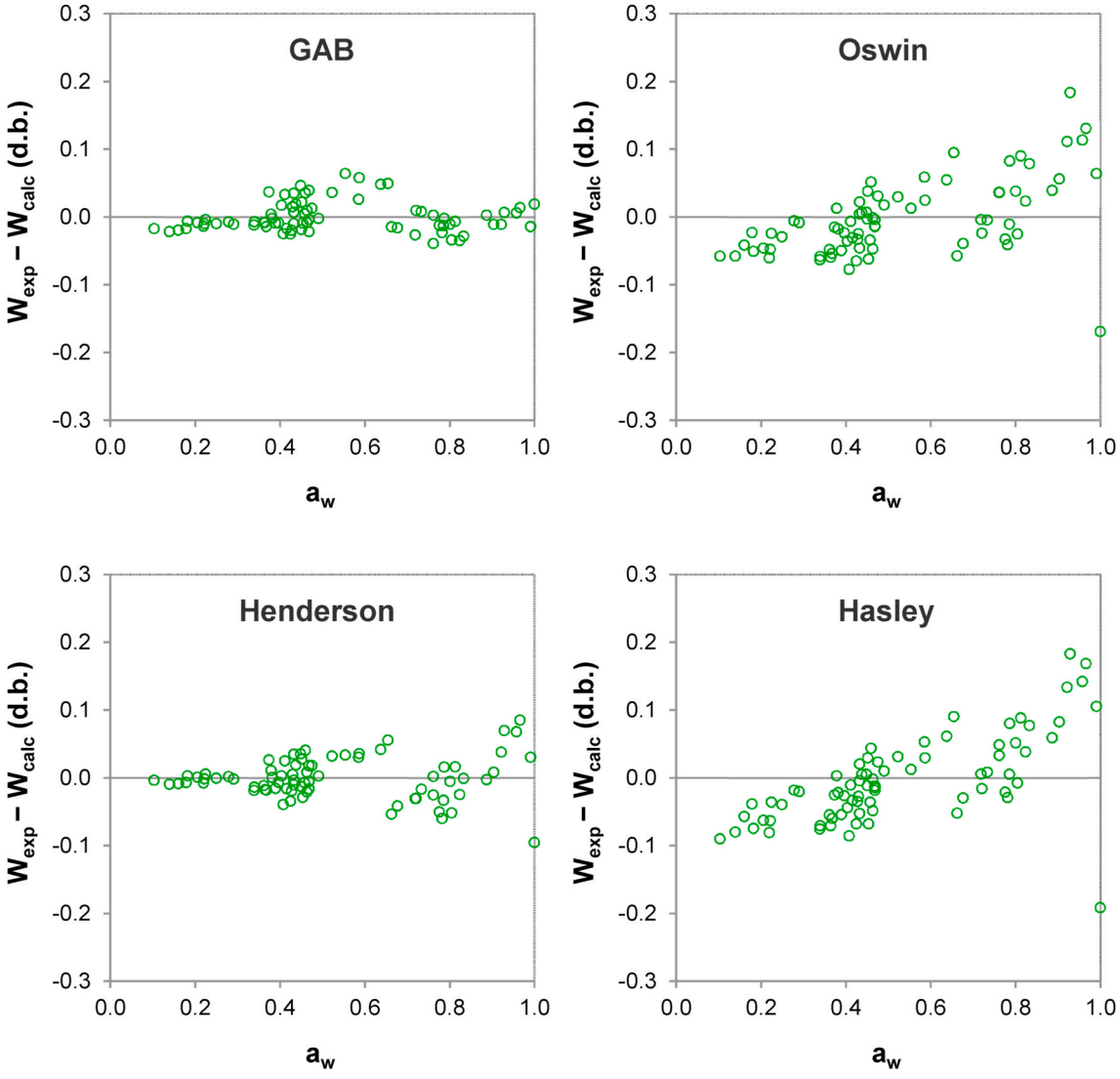

Fig. 2. Residual plots for the GAB, Oswin, Henderson and Halsey models.

GAB model, providing a better differentiation of the curves at the different temperatures. However, VAR reached by Henderson model (94.0%) was slightly lower than for GAB equation (96.6%). Taking into account the high experimental variability, the VAR values provided by GAB and Henderson model could be considered appropriate. In the case of Ratti model, a minimal influence of temperature is observed on the computed curves, which absolutely disappears at water activities higher than 0.5. This fact explains the low VAR reached by the Ratti model (90.9%).

When choosing one model for the mathematical description of isotherms, it is also recommended to consider other aspects, such as the lowest number of parameters and its physical meaning. A small number of parameters for modeling purposes increases the degrees of freedom in the identification procedure. Furthermore, the physical meaning of the parameters contributes to better interpret and understand the physical phenomenon being described and allows comparisons with other

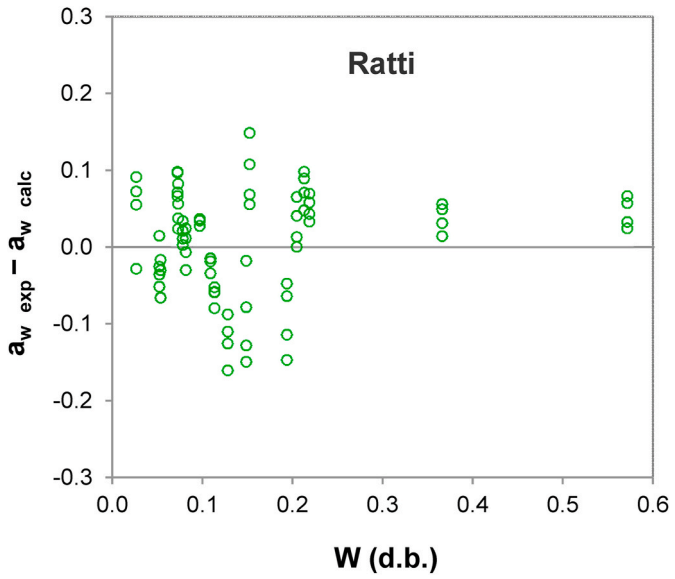

Fig. 3. Plot of residual for the Ratti model.

materials (García-Pérez et al., 2008). Therefore, it seems that GAB is the most adequate equation for modeling the desorption isotherms of pork liver since it provided the best fit and its parameters have a physical meaning. Nevertheless, the Henderson model can be recommended in those cases in which a lower number of parameters are required.

Based on the theoretical definition of the GAB model, the identified value of ΔH_C ($1.07{\cdot}10^4$ kJ kmol^{-1}) indicates that the binding energy between the water molecules of the monolayer and the food matrix was considerably higher than the binding energy of the water molecules of the multilayer. Clemente et al. (2009) reported a smaller difference between the monolayer (H_m) and multilayer (H_n) heat of sorption for raw pork meat. On the other hand, the latent heat of vaporization of water (L_v) was slightly higher than the binding energy in the multilayer as a consequence of the estimated value of ΔH_K ($6.51{\cdot}10^2$ kJ kmol^{-1}), which reflects once again the limited interaction of the water molecules with the solid matrix at high moisture contents.

3.3. Thermodynamic properties

The isosteric heat of desorption for pork liver was computed using two different methodologies (Eqs. (11) and (12)) based on the Clausius-Clapeyron equation (Eq. (10)). By means of the GAB model, the desorption isotherms were estimated and used, via interpolation, to obtain water activity values at the different experimental temperatures for a constant moisture content. Fig. 5 shows the isosteric heat of desorption as a function of moisture content for the graphical and integral methods. The four experimental temperatures were used for the graphical procedure (Eq. (11)), while the integral procedure (Eq. (12)) only needed the two extreme conditions, 0 and 50 °C. It can be seen that both curves were very close over the whole moisture range. According to Iglesias et al. (1989) this would indicate that the net isosteric heat of sorption for pork liver could be considered to be non-dependent on the temperature. In Fig. 5, two zones can be distinguished: (i) for moisture contents higher than 0.15 d.b., the isosteric heat remained almost constant with an average difference of $7.29{\cdot}10^2 \pm 74.88$ kJ kmol^{-1} with respect to the latent heat of vaporization of water ($4.39{\cdot}10^4$ kJ kmol^{-1}, average value between 0 and 50 °C). When working with raw pork and goat meat, respectively Clemente et al. (2009) and Singh et al. (2006) also found the limit between these two zones at a moisture content of 0.15 d b. (ii) For the low moisture content zone, lower than 0.15 d.b., the isosteric heat increased sharply as the water content was reduced, reaching a value of $5.34{\cdot}10^4$ kJ kmol^{-1} for the lowest moisture content

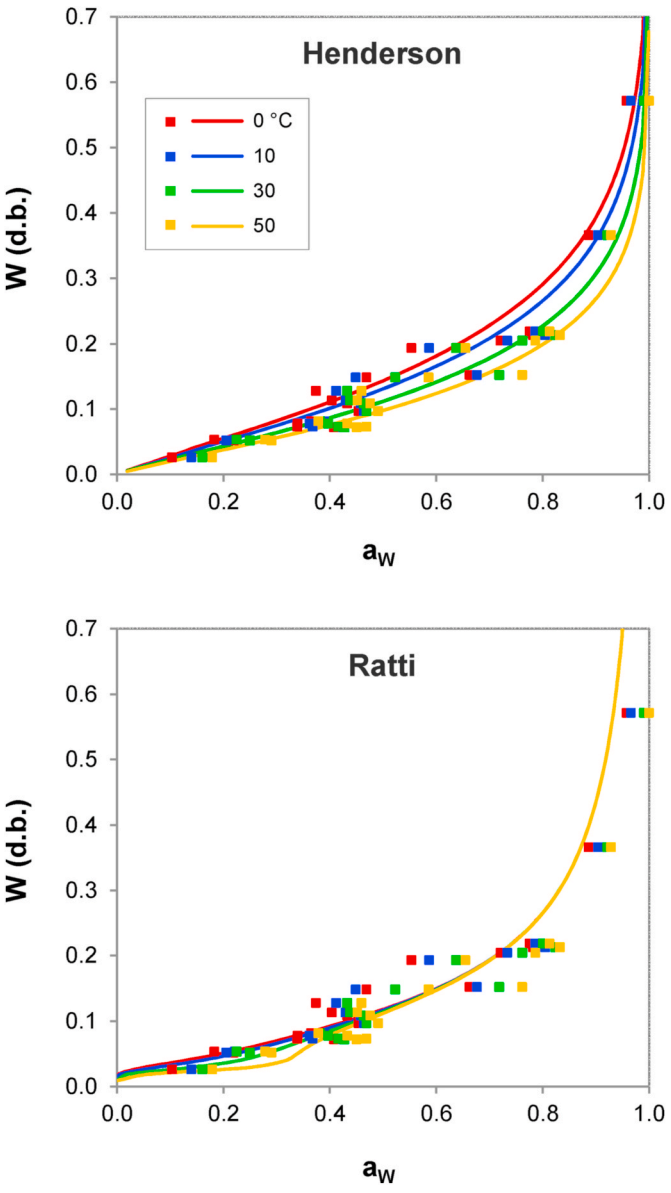

Fig. 4. Experimental desorption isotherms of pork liver and Henderson and Ratti models at 0, 10, 30 and 50 °C.

in this study. The sharp increase in the isosteric heat at the end of the desorption process is explained by the fact that water molecules are bound to the higher energy sites (Al-Muhtaseb et al., 2002). The following isosteric heats ($\times 10^4$ kJ kmol^{-1}) have been reported for low moisture contents in: goat, 44.64 (Singh et al., 2006), beef, 8.55 (Ahmat et al., 2014), anchovy, 7.50 (Moraes & Pinto, 2012), shrimp, 6.69 (Shi et al., 2016) and pork, 6.41 (Clemente et al., 2009). The fact that the isosteric heat for the pork liver is lower than that of these products indicates that the pork liver requires less energy than other protein matrices to remove tightly bound water.

The isosteric heat of desorption was also calculated from the Riedel equation (Eq. (14)). The estimated parameters were $A_r = 1620.63$ K and $B_r = 14.83$ kg dry solid·(kg water)$^{-1}$, and the VAR was 96.4%. From moisture contents higher than 0.15 d.b., the isosteric heat computed from the Riedel equation was closer to the latent heat of vaporization of the water than the figures obtained from the Clausius-Clapeyron equation (Fig. 5). Despite this fact, for low moisture contents (lower than 0.15 d.b.), the Riedel curve was close to the values estimated by the graphical and integral procedures.

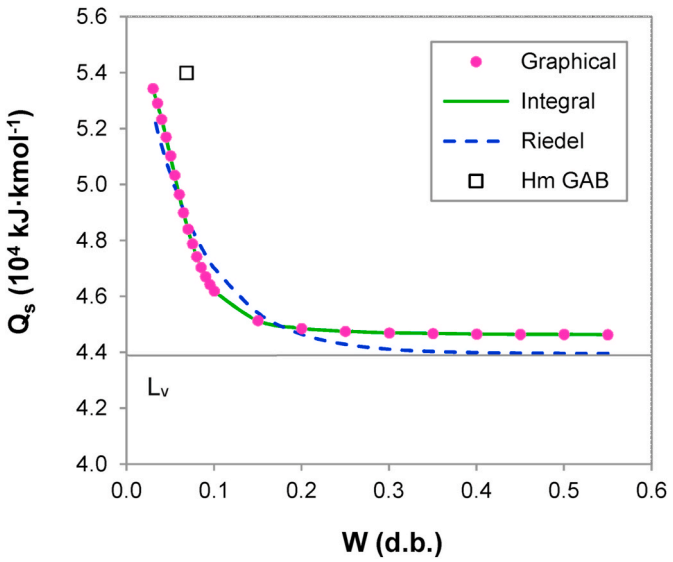

Fig. 5. Influence of moisture content on estimated isosteric heat of desorption.

From the identified parameters of the GAB model (Table 3), the monolayer heat of sorption was calculated from Eq. (2), $H_m = 5.40{\cdot}10^4$ kJ kmol^{-1}. This figure was compared with the isosteric heat estimated ($4.87{\cdot}10^4 \pm 140.22$ kJ kmol^{-1}) at the monolayer moisture content ($W_m = 0.068$ d.b.), considering the graphical, integral and Riedel procedures (Fig. 5). Therefore, the average difference found with respect to H_m was 9.84 ± 0.26%, probably due to the variability associated with the experimental desorption data (Chirife & Iglesias, 1992).

The desorption entropy was obtained from the isosteric heat estimated using Eq. (17) for each experimental temperature (Fig. 6). As can be seen, there was great similarity between the identified entropy values at the different experimental temperatures analyzed. Thus, the moisture content of 0.15 d.b. Again separates two differentiated regions in Fig. 6: (i) for moisture levels of under 0.15 d.b., the desorption entropy exhibited a steep increase as the moisture content was reduced, since the water molecules are being removed from the higher energy sites and, therefore, the availability of strong sorption sites is increased; (ii) however, for moisture contents higher than 0.15 d.b., the desorption entropy declined slightly as the moisture content was reduced, which could be ascribed to the reduction in the degree of freedom of the water molecules adsorbed on the multilayer as a result of the progressive dehydration of the solid matrix. Similar trends have previously been reported for high-protein products, such as crayfish (Ariahu, Kaze, & Achem, 2006), shrimp (Shi et al., 2016), anchovy (Moraes & Pinto, 2012) or sucuk (a dry-fermented Turkish sausage) (Polatoğlu, Beşe, Kaya, & Aktaş, 2011), as well as for different dairy protein concentrates (Sawhney, 2011; Sawhney, Sarkar, Patil, & Sharma, 2014; Seth, Dash, Mishra, & Deka, 2018).

Fig. 7 illustrates the gradual increase in the Gibbs energy that takes place as the moisture content decreases. As for the entropy, the computed curves at each experimental temperature completely overlap. For moisture contents lower than 0.15 d.b., the Gibbs energy exhibits a steep increase, which is linked to a stronger affinity between the water and sorbent material. This is consistent with the behavior observed for the isosteric heat and the entropy. Thus, the increasing trend of the Gibbs energy as the moisture content decreases has also been found in the desorption of others food matrices (Oliveira, Correa, Oliveira, Reis, & Devilla, 2017; Oliveira, Correa, Santos, Casanova, & Diniz, 2011; Shaik & Kailappan, 2007). However, the cited works reported a clear temperature-dependent on the Gibbs energy. Specifically, for a given moisture content, the Gibbs energy decreased as the temperature increased, due to a lower sorbent affinity for the water molecules as temperature rises. In contrast, in Fig. 7, the curves at the different temperature almost overlap, which confirms the mild temperature effect found on desorption isotherms in pork liver. Moreover, it has to be clarified that the positive Gibbs energy values denote a non-spontaneous phenomenon ($\Delta G>0$), solely as a result of how Eq. (15) is commonly used for desorption processes.

4. Conclusions

The desorption isotherms for pork liver have been obtained experimentally at 0, 10, 30 and 50 °C over a wide range of water activity. Water activity figures of under 1 only appeared when the moisture content was under 36% (w.b.), which confirms the high availability of water in pork liver, and explains the rapid and easy degradation of this food material. Of the five models tested for the mathematical description of the desorption isotherms, the GAB model was the most adequate since it provided the highest explained variance, showed a random residual

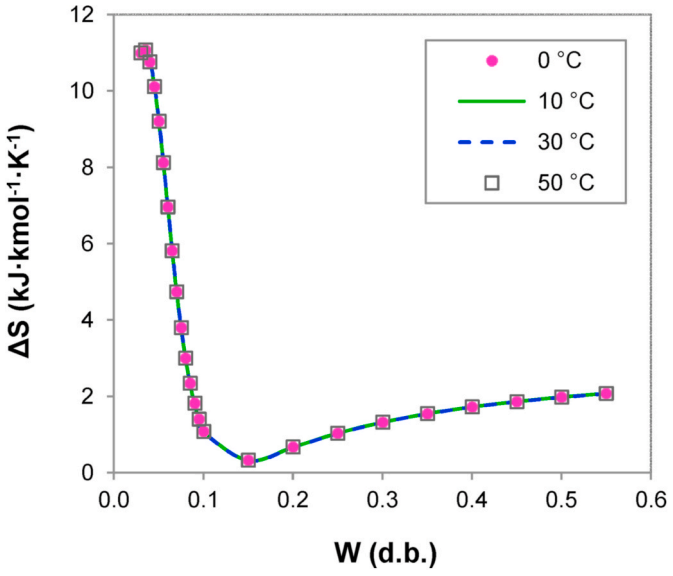

Fig. 6. Influence of moisture content on estimated desorption entropy at 0, 10, 30 and 50 °C.

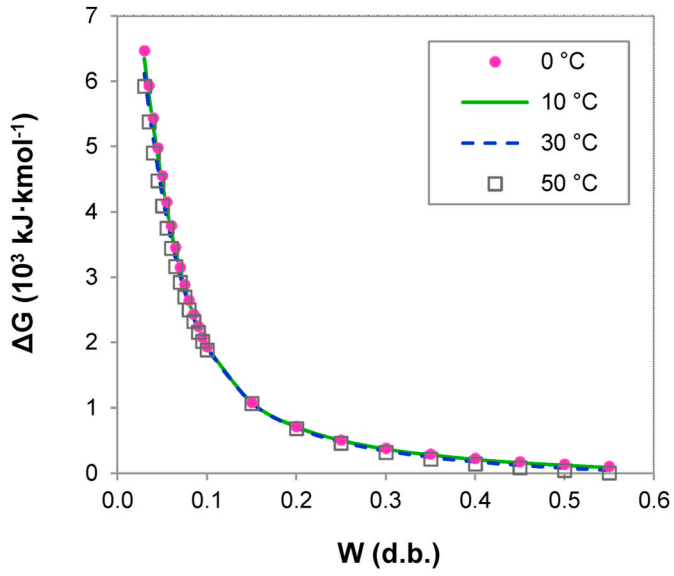

Fig. 7. Influence of moisture content on estimated Gibbs energy at 0, 10, 30 and 50 °C.

distribution and contributed to the physical description of the desorption process. The Henderson model could be an alternative when a low number of fitting parameters are required and the Ratti model could be used in those cases in which an explicit form for the water activity is sought.

The computed figures of the isosteric heat, entropy and Gibbs energy for the desorption process reflected that, at low moisture contents (lower than 0.15 d.b.), the fact that a large amount of energy is required for the removal of water molecules is due to the high water-sorbent affinity, as a consequence of a considerable availability of strong sorption sites.

The experimental desorption isotherms reported in this work, as well as the modeling results, constitute a valuable tool for the design of drying processes in order to stabilize a highly perishable foodstuff, such as pork liver. The analysis of the drying process is essential for the further research addressing the extraction of the protein fraction of pork liver from the dried product, a reasonable strategy considering the demand of protein materials and the high-environmental impact of meat industry. Further studies should also investigate the adsorption process in the dry material as a means of optimizing storage conditions while minimizing spoilage risks.

CRediT authorship contribution statement

E.A. Sánchez-Torres: Software, Formal analysis, Writing – original draft. **B. Abril:** Investigation, Formal analysis, Writing – original draft. **J. Benedito:** Conceptualization, Writing – review & editing. **J. Bon:** Conceptualization, Validation, Writing – review & editing. **J.V. García-Pérez:** Conceptualization, Supervision, Methodology, Writing – review & editing.

Declaration of competing interest

None.

Acknowledgements

The authors acknowledge the financial support from the "Ministerio de Economía y Competitividad (MINECO)" and "Instituto Nacional de Investigación y Tecnología Agraria y Alimentaria (INIA)" in Spain (Project RTA 2017-00024-C04-03). Eduardo A. Sanchez-Torres acknowledges the FPU PhD contract (FPU18/01439) granted by the Spanish Ministry of Science, Innovation and Universities.

Nomenclature

a	Antoine equation parameter, dimensionless
a_w	Water activity, dimensionless
A_H	Henderson model parameter, $(\text{kg dry solid (kg water K)}^{-1})^{B_H}$
A_{Ha}	Hasley model parameter, dimensionless
A_{Os}	Oswin model parameter, kg water·(kg dry solid)$^{-1}$
A_r	Riedel model parameter, K
b	Antoine equation parameter, K
B_H	Henderson model parameter, dimensionless
B_{Ha}	Hasley model parameter, K^{-1}
B_{Os}	Oswin model parameter, kg water·(kg dry solid·K)$^{-1}$
B_r	Riedel model parameter, kg dry solid·(kg water)$^{-1}$
c	Antoine equation parameter, K
C	GAB model parameter, dimensionless
C_H	Henderson model parameter, K
C_{Ha}	Hasley model parameter, dimensionless
C_0	GAB model parameter, dimensionless
C_{Os}	Oswin model parameter, dimensionless
d.b.	Dry basis, kg·(kg dry solid)$^{-1}$
F_{obj}	Objective function for optimization procedure, units of the squared estimation
H_m	Monolayer sorption heat, kJ·kmol^{-1}
H_n	Multilayer sorption heat, kJ·kmol^{-1}
k_i	Ratti model parameter ($1 \leq i \leq 5$)
K	GAB model parameter, dimensionless
K_0	GAB model parameter, dimensionless
L_v	Latent heat of vaporization of water, kJ·kmol^{-1}
m	Number of model parameters
n	Number of data points
P_s	Saturation vapor pressure, Pa
Q_s	Isosteric heat of sorption, kJ·kmol^{-1}
q_{sn}	Net isosteric heat of sorption, kJ·kmol^{-1}
R	Universal gas constant, kJ·(kmol·K)$^{-1}$
S_y	Standard deviation of the sample, units of the sample
S_{yx}	Standard deviation of the estimation, units of the estimation
T	Temperature, K
VAR	Percentage of explained variance, %
W	Average equilibrium moisture content, kg water·(kg dry solid)$^{-1}$
w.b.	Wet basis, kg·(kg wet solid)$^{-1}$
W_m	Monolayer average equilibrium moisture content, kg water·(kg dry solid)$^{-1}$
$y_{i\ calc}$	Value i predicted by the model, units of the estimation
$y_{i\ exp}$	Measured value i, units of the sample

$\overline{y_{exp}}$	Average measured value, units of the sample
ΔH_C	GAB model parameter, kJ·kmol^{-1}
ΔH_K	GAB model parameter, kJ·kmol^{-1}
ΔG	Change in Gibbs free energy, kJ·kmol^{-1}
ΔH	Change in sorption enthalpy, kJ·kmol^{-1}
ΔS	Change in sorption entropy, kJ·(kmol·K)$^{-1}$

References

Ahmat, T., Bruneau, D., Kuitche, A., & Aregba, A. W. (2014). Desorption isotherms for fresh beef: An experimental and modeling approach. *Meat Science, 96*(4), 1417–1424.

Al-Muhtaseb, A. H., McMinn, W. A. M., & Magee, T. R. A. (2002). Moisture sorption isotherm characteristics of food products: A review. *Food and Bioproducts Processing, 80*(2), 118–128. https://doi.org/10.1205/09603080252938753

Al-Muhtaseb, A. H., McMinn, W. A. M., & Magee, T. R. A. (2004). Water sorption isotherms of starch powders: Part 1: Mathematical description of experimental data. *Journal of Food Engineering, 61*(3), 297–307. https://doi.org/10.1016/S0260-8774(03)00133-X

Anderson, R. B. (1946). Modifications of the brunauer, emmett and teller Equation1. *Journal of the American Chemical Society, 68*(4), 686–691. https://doi.org/10.1021/ja01208a049

Aoac. (2019). *Official methods of analysis of AOAC International* (21st ed.). Gaithersburg: Maryland (AOAC International).

Ariahu, C. C., Kaze, S. A., & Achem, C. D. (2006). Moisture sorption characteristics of tropical fresh water crayfish (Procambarus clarkii). *Journal of Food Engineering, 75*(3), 355–363. https://doi.org/10.1016/j.jfoodeng.2005.03.062

Aykın-Dinçer, E., & Erbaş, M. (2018). Drying kinetics, adsorption isotherms and quality characteristics of vacuum-dried beef slices with different salt contents. *Meat Science, 145*, 114–120.

Babicz, M., Kropiwiec-Domańska, K., Szyndler-Nędza, M., Grzebalska, A. M., Łuszczewska-Sierakowska, I., Wawrzyniak, A., et al. (2018). Physicochemical parameters of selected internal organs of fattening pigs and wild boars. *Annals of Animal Science, 18*(2), 575–591.

Betiol, L. F. L., Evangelista, R. R., Sanches, M. A. R., Basso, R. C., Gullón, B., Lorenzo, J. M., et al. (2020). Influence of temperature and chemical composition on water sorption isotherms for dry-cured ham. *LWT, 123*, 109112.

Brunauer, S., Deming, L. S., Deming, W. E., & Teller, E. (1940). On a theory of the van der Waals adsorption of gases. *Journal of the American Chemical Society, 62*(7), 1723–1732.

Chen, C. C. (1988). *A study of equilibrium relative humidity for Yellow-dent corn Kernels*. University of Minnesota. Retrieved from https://books.google.es/books?id=7PQpBrWxVQUC.

Chen, C. (2006). Obtaining the isosteric sorption heat directly by sorption isotherm equations. *Journal of Food Engineering, 74*(2), 178–185. https://doi.org/10.1016/j.jfoodeng.2005.01.041

Chen, C.-C., & Morey, R. V. (1989). Comparison of four EMC/ERH equations. *Transactions of the ASAE, 32*(3), 983–990.

Chirife, J., & Iglesias, H. A. (1992). Estimation of the precision of isosteric heats of sorption determined from the temperature dependence of food isotherms. *LWT-Food Science and Technology, 25*(1), 83–84.

Clemente, G., Bon, J., Benedito, J., & Mulet, A. (2009). Desorption isotherms and isosteric heat of desorption of previously frozen raw pork meat. *Meat Science, 82*(4), 413–418. https://doi.org/10.1016/j.meatsci.2009.02.020

Comaposada, J., Gou, P., & Arnau, J. (2000). The effect of sodium chloride content and temperature on pork meat isotherms. *Meat Science, 55*(3), 291–295. https://doi.org/10.1016/s0309-1740(99)00154-0

De Maere, H., Chollet, S., Claeys, E., Michiels, C., Govaert, M., De Mey, E., et al. (2017). In vitro zinc protoporphyrin IX formation in different meat sources related to potentially important intrinsic parameters. *Food and Bioprocess Technology, 10*(1), 131–142.

Delgado, A. E., & Sun, D.-W. (2002a). Desorption isotherms and glass transition temperature for chicken meat. *Journal of Food Engineering, 55*(1), 1–8. https://doi.org/10.1016/S0260-8774(01)00222-9

Delgado, A. E., & Sun, D.-W. (2002b). Desorption isotherms for cooked and cured beef and pork. *Journal of Food Engineering, 51*(2), 163–170. https://doi.org/10.1016/S0260-8774(01)00053-X

Fakhfakh, R., Mihoubi, D., & Kechaou, N. (2018). Moisture sorption isotherms and thermodynamic properties of bovine leather. *Heat and Mass Transfer, 54*(4), 1163–1176.

Fontana, A. J., Jr., & Carter, B. P. (2020, April 17). Measurement of water activity, moisture sorption isotherm, and moisture content of foods. *Water Activity in Foods*. https://doi.org/10.1002/9781118765982.ch8

García-Pérez, J. V., Cárcel, J. A., Clemente, G., & Mulet, A. (2008). Water sorption isotherms for lemon peel at different temperatures and isosteric heats. *Lebensmittel-Wissenschaft und -Technologie- Food Science and Technology, 41*(1), 18–25. https://doi.org/10.1016/j.lwt.2007.02.010

Goula, A. M., Karapantsios, T. D., Achilias, D. S., & Adamopoulos, K. G. (2008). Water sorption isotherms and glass transition temperature of spray dried tomato pulp. *Journal of Food Engineering, 85*(1), 73–83. https://doi.org/10.1016/j.jfoodeng.2007.07.015

Green, D. D. W., & Southard, D. M. Z. (2019). *Perry's Chemical Engineers' Handbook* (9th ed.). New York: McGraw-Hill (Education).

Haque, A., Shimizu, N., Kimura, T., & Bala, B. K. (2007). Net isosteric heats of adsorption and desorption for different forms of hybrid rice. *International Journal of Food Properties, 10*(1), 25–37. https://doi.org/10.1080/10942910600613228

Iglesias, H. A., & Chirife, J. (1976). Prediction of the effect of temperature on water sorption isotherms of food material. *International Journal of Food Science and Technology, 11*(2), 109–116.

Iglesias, H. A., & Chirife, J. (1982). *Handbook of food isotherms: Water sorption parameters for food and food components*.

Iglesias, H. A., Chirife, J., & Fontan, C. F. (1989). On the temperature dependence of isosteric heats of water sorption in dehydrated foods. *Journal of Food Science, 54*(6), 1620–1623. https://doi.org/10.1111/j.1365-2621.1989.tb05174.x

Kabil, E., Aktaş, N., & Balcı, E. (2012). Effect of sodium chloride, sodium nitrite and temperature on desorption isotherms of previously frozen beef. *Meat Science, 90*(4), 932–938. https://doi.org/10.1016/j.meatsci.2011.11.035

Kaleemullah, S., & Kailappan, R. (2004). Moisture sorption isotherms of red chillies. *Biosystems Engineering, 88*(1), 95–104. https://doi.org/10.1016/j.biosystemseng.2004.01.003

Kaymak-Ertekin, F., & Gedik, A. (2004). Sorption isotherms and isosteric heat of sorption for grapes, apricots, apples and potatoes. *Lebensmittel-Wissenschaft und -Technologie-Food Science and Technology, 37*(4), 429–438. https://doi.org/10.1016/j.lwt.2003.10.012

Khalloufi, S., Giasson, J., & Ratti, C. (2000). Water activity of freeze dried mushrooms and berries. *Canadian Agricultural Engineering, 42*(1), 51–56.

Khiari, R., Zemni, H., Maury, C., & Mihoubi, D. (2020). Modeling desorption isotherms and thermodynamic properties of Italia grapes. *Journal of Food Processing and Preservation*.

Kiani, H., & Sun, D.-W. (2011). Water crystallization and its importance to freezing of foods: A review. *Trends in Food Science & Technology, 22*(8), 407–426. https://doi.org/10.1016/j.tifs.2011.04.011

Lafarga, T., & Hayes, M. (2014). Bioactive peptides from meat muscle and by-products: Generation, functionality and application as functional ingredients. *Meat Science, 98*(2), 227–239. https://doi.org/10.1016/j.meatsci.2014.05.036

Lee, S. Y., Yoon, S. Y., Kim, O. Y., Kim, H. S., Jung, E. Y., Koh, K. C., et al. (2020). Development of batch processing to obtain bioactive materials from pork byproducts. *Animal Production Science, 60*(2), 316–322.

Lipson, C., & Sheth, N. J. (1973). *Statistical design and analysis of Engineering experiments*. McGraw-Hill. Retrieved from https://books.google.es/books?id=2YpRAAAAMAAJ.

Mbarek, R., & Mihoubi, D. (2019). Thermodynamic properties and water desorption isotherms of Golden Delicious apples. *Heat and Mass Transfer/Waerme- Und Stoffuebertragung, 55*(5), 1405–1418. https://doi.org/10.1007/s00231-018-2527-8

Menkov, N. D. (2000). Moisture sorption isotherms of vetch seeds at four temperatures. *Journal of Agricultural Engineering Research, 76*(4), 373–380. https://doi.org/10.1006/jaer.2000.0551

Moraes, K., & Pinto, L. A. A. (2012). Desorption isotherms and thermodynamics properties of anchovy in natura and enzymatic modified paste. *Journal of Food Engineering, 110*(4), 507–513. https://doi.org/10.1016/j.jfoodeng.2012.01.012

Mora, L., Reig, M., & Toldrá, F. (2014). Bioactive peptides generated from meat industry by-products. *Food Research International, 65*, 344–349. https://doi.org/10.1016/j.foodres.2014.09.014

Mulet, A., García-Pascual, P., Sanjuán, N., & García-Reverter, J. (2002). Equilibrium isotherms and isosteric heats of morel (Morchella esculenta). *Journal of Food Engineering, 53*(1), 75–81. https://doi.org/10.1016/S0260-8774(01)00142-X

Oliveira, G., Correa, P., Oliveira, A., Reis, R., & Devilla, I. (2017). Application of GAB model for water desorption isotherms and thermodynamic analysis of sugar beet seeds. *Journal of Food Process Engineering, 40*, 1–8. https://doi.org/10.1111/jfpe.12278

Oliveira, G., Correa, P., Santos, E., Casanova, P., & Diniz, M. (2011). Evaluation of thermodynamic properties using GAB model to describe the desorption process of cocoa beans. *International Journal of Food Science and Technology, 46*, 2077–2084. https://doi.org/10.1111/j.1365-2621.2011.02719.x

Peng, G., Chen, X., Wu, W., & Jiang, X. (2007). Modeling of water sorption isotherm for corn starch. *Journal of Food Engineering, 80*(2), 562–567. https://doi.org/10.1016/j.jfoodeng.2006.04.063

Polatoğlu, B., Beşe, A. V., Kaya, M., & Aktaş, N. (2011). Moisture adsorption isotherms and thermodynamics properties of sucuk (Turkish dry-fermented sausage). *Food and Bioproducts Processing, 89*(4), 449–456. https://doi.org/10.1016/j.fbp.2010.06.003

Poling, B. E., Prausnitz, J. M., & O'Connell, J. P. (2001). *Properties of Gases and Liquids* (5th ed.). New York: McGraw-Hill. Education. Retrieved from https://www.accessengineeringlibrary.com/content/book/9780070116825.

Ponwiboon, N., & Rojanakorn, T. (2017). Desorption isotherms and drying characteristics of Nile tilapia fish sheet. *International Food Research Journal, 24*(3).

Riedel, L. (1977). Calorimetric measurements of heats of hydration of foods. *Chemie Microbiologie Und Technologie Der Lebensmittel, 5*(97), 101.

Rizvi, S. S. (2014). Thermodynamic properties of foods in dehydration. *Engineering properties of foods* (4th ed.). Boca Raton: CRC Press. https://doi.org/10.1201/b16897

Robertson, G. L., & Lee, D. S. (2021). Comparison of linear and GAB isotherms for estimating the shelf life of low moisture foods packaged in plastic films. *Journal of Food Engineering, 291*. https://doi.org/10.1016/j.jfoodeng.2020.110317, 110317.

Sahu, S. N., Tiwari, A., Sahu, J. K., Naik, S. N., Baitharu, I., & Kariali, E. (2018). Moisture sorption isotherms and thermodynamic properties of sorbed water of chironji (Buchanania lanzan Spreng.) kernels at different storage conditions. *Journal of Food Measurement and Characterization, 12*(4), 2626–2635. https://doi.org/10.1007/s11694-018-9880-7

Sarwar, M. I., Hussain, M. S., & Leghari, A. R. (2013). Heparin can be isolated and purified from bovine intestine by different techniques. *International Journal of Pharmaceutical Science Invention, 2*, 21–25.

Sawhney, I. K. (2011). Characterizing the engineering properties of skim milk powder and protein derivatives of Buffalo milk. *Sant Longowal*. Retrieved from http://hdl.handle.net/10603/3306.

Sawhney, I. K., Sarkar, B. C., Patil, G. R., & Sharma, H. K. (2014). Moisture sorption isotherms and thermodynamic properties of whey protein concentrate powder from buffalo skim milk. *Journal of Food Processing and Preservation, 38*(4), 1787–1798. https://doi.org/10.1111/jfpp.12148

Seong, P. N., Park, K. M., Cho, S. H., Kang, S. M., Kang, G. H., Park, B. Y., et al. (2014). Characterization of edible pork by-products by means of yield and nutritional composition. *Korean Journal for Food Science of Animal Resources, 34*(3), 297–306. https://doi.org/10.5851/kosfa.2014.34.3.297

Seth, D., Dash, K. K., Mishra, H. N., & Deka, S. C. (2018). Thermodynamics of sorption isotherms and storage stability of spray dried sweetened yoghurt powder. *Journal of Food Science & Technology, 55*(10), 4139–4147. https://doi.org/10.1007/s13197-018-3340-6

Shaik, K., & Kailappan, R. (2007). Monolayer moisture, free energy change and fractionation of bound water of red chillies. *Journal of Stored Products Research, 43*, 104–110. https://doi.org/10.1016/j.jspr.2005.12.001

Shi, Q., Lin, W., Zhao, Y., Zhang, P., & Wang, R. (2016). Moisture adsorption isotherms and thermodynamic properties of Penaeus vannamei meat with and without maltodextrin addition. *Journal of Aquatic Food Product Technology, 25*(8), 1348–1367.

Singh, R. R. B., Rao, K. H., Anjaneyulu, A. S. R., & Patil, G. R. (2006). Water desorption characteristics of raw goat meat: Effect of temperature. *Journal of Food Engineering, 75*(2), 228–236. https://doi.org/10.1016/j.jfoodeng.2005.04.013

Staudt, P. B., Tessaro, I. C., Marczak, L. D. F., Soares, R., de, P., & Cardozo, N. S. M. (2013). A new method for predicting sorption isotherms at different temperatures: Extension to the GAB model. *Journal of Food Engineering, 118*(3), 247–255. https://doi.org/10.1016/j.jfoodeng.2013.04.013

Steen, L., Glorieux, S., Goemaere, O., Brijs, K., Paelinck, H., Foubert, I., et al. (2016). Functional properties of pork liver protein fractions. *Food and Bioprocess Technology, 9*(6), 970–980.

Taormina, P. J., & Sofos, J. N. (2014). *Low-water activity meat products BT - the microbiological Safety of low water activity foods and Spices*. In J. B. Gurtler, M. P. Doyle, & J. L. Kornacki (Eds.). New York, NY: Springer. https://doi.org/10.1007/978-1-4939-2062-4_9. New York.

Thompson, T. L., Peart, R. M., & Foster, G. H. (1968). Mathematical simulation of corn drying - a new model. *Transaction of the ASAE, 11*(4), 582–586.

Toldrá, F., Mora, L., & Reig, M. (2016). New insights into meat by-product utilization. *Meat Science, 120*, 54–59. https://doi.org/10.1016/j.meatsci.2016.04.021

Toujani, M., Hassini, L., Azzouz, S., & Belghith, A. (2011). Drying characteristics and sorption isotherms of silverside fish (Atherina). *International Journal of Food Science and Technology, 46*(3), 594–600.

Wakamatsu, J., Murakami, N., & Nishimura, T. (2015). A comparative study of zinc protoporphyrin IX-forming properties of animal by-products as sources for improving the color of meat products. *Animal Science Journal, 86*(5), 547–552. Retrieved from https://www.unboundmedicine.com/medline/citation/25441257/A_comparative_study_of_zinc_protoporphyrin_IX_forming_properties_of_animal_by_products_as_sources_for_improving_the_color_of_meat_products_.

Yogendrarajah, P., Samapundo, S., Devlieghere, F., De Saeger, S., & De Meulenaer, B. (2015). Moisture sorption isotherms and thermodynamic properties of whole black peppercorns (Piper nigrum L.). *LWT-Food Science and Technology, 64*(1), 177–188.

Yoon, S. Y., Da Young Lee, O. Y. K., Lee, S. Y., & Hur, S. J. (2018). Development of commercially viable method of conjugated linoleic acid synthesis using linoleic acid fraction obtained from pork by-products. *Korean Journal for Food Science of Animal Resources, 38*(4), 693.